

Removal of sulfamethoxazole in aqueous solution by two activated carbons from secondary sludge and biomass

C.E. Rodríguez-Martínez^a, E. Gutiérrez Segura^{a,*}, C. Fall^b, A. Colín-Cruz^a

^aUniversidad Autónoma del Estado de México, Facultad de Química, Paseo Colón esq. Paseo Tollocan, S/N. C.P. 50180, Toluca, México, emails: eegutierrez@uaemex.mx (E. Gutiérrez Segura), maye.eve@hotmail.com (C.E. Rodríguez-Martínez), acolinc@uaemex.mx (A. Colín-Cruz)

^bCentro Interamericano de Recursos del Agua CIRA-UAEM, Carretera Toluca-Ixtlahuaca Km. 14.5, Unidad San Cayetano, Toluca, Estado de México, México, email: cfall@uaemex.mx

Received 26 October 2018; Accepted 27 March 2019

ABSTRACT

Removal behavior of sulfamethoxazole (SMX) by two carbonaceous materials was studied. The adsorbents were obtained by pyrolysis (550°C, 1 h under nitrogen flow), followed by acid washing of residuals consisting of a biological secondary sludge (SSCM) and a local herbaceous plant (*Phragmites communis*, RCM). The morphology, elemental composition and chemical properties of the obtained carbonaceous materials were fully characterized. The equilibrium and kinetics of SMX adsorption were studied and modelled, together with the pH and temperature effects. Additional heating of the materials under limited aerobic conditions (800°C, 1 h) improved their adsorption capacity, compared with simple pyrolysis at 550°C only. The uptake rates followed a second-order model, while the adsorption capacities (up to 30.4 and 21.5 mg g⁻¹) were predictable with Freundlich and Langmuir isotherms (heterogeneous vs. homogeneous adsorption, on SSCM and RCM, respectively). Removal of sulfamethoxazole was most effective at acidic pH in both materials. The thermodynamic parameters (ΔG° , ΔH° , ΔS°) indicated that SMX adsorption was spontaneous, favorable, exothermic and reversible. The residuals were turned into promising low-cost sorbents for removal of sulfamethoxazole from water.

Keywords: Antibiotics; Sorption; Sulfamethoxazole; Sludge; Sorbents

1. Introduction

Recent research has focused on the elimination of a group of so-called emerging pollutants; because their presence has been documented inclusive in both wastewater and treated water [1,2]. Within this group are drugs such as antibiotics. Antibiotics are used worldwide in great amounts. The annual consumption was estimated between 100,000 and 200,000 tons [3]. Antibiotics are classified as bio-accumulative compounds and are thus regarded as hazardous chemicals that contaminate the aquatic and terrestrial ecosystems [4].

The sulfamethoxazole (SMX) is a sulfa drug, which belongs to the sulfonamide group and contains a 4-amino phenylsulfonylamide core structure. The sulfamethoxazole (4-amino-N-5-methylisoxazol-3-yl-benzenesulfonamide) is widely used for the control of human infections (urinary, respiratory and gastrointestinal) [5]. Part of the ingested mass is excreted as primary or secondary metabolites. 10% to 30% of the ingested SMX dose is excreted via urine in its original form [6]. In fact, SMX has been detected in the range of ng L⁻¹ to mg L⁻¹ in surface waters [7]. Hence the importance of their elimination from the water bodies, since the chronic exposure can lead to the development

* Corresponding author.

of antibiotic resistance; therefore, improving the removal technologies is a priority [8].

Unfortunately, many pharmaceutical compounds are not completely removed by wastewater treatment plants (WWTPs) and consequently they have been detected around the world in WWTPs effluents, surface waters and, less frequently, in ground and drinking waters [4]. The elimination efficiency of antibiotics by wastewater treatment facilities varies greatly between 20% and 90%, depending on the processes employed [9]. For SMX, the removal efficiencies at the WWTPs are reported to be between 24% and 36% [8].

Several methods have been investigated to remove pharmaceuticals from contaminated water, such as by biodegradation, photocatalysis, ozonation, Fenton process, advanced oxidation processes (AOPs) and adsorption [4,10]. AOPs are efficient treatments to degrade pharmaceuticals, however various intermediates can be generated due to partial oxidation of the complex compounds, leading to toxicity that can be even higher than for the original contaminants [4]. In addition, AOPs are very expensive and operationally complex for complete degradation of recalcitrant compounds [11]. In contrast, adsorption is one of the most promising processes, since it is efficient, simple to design, relatively inexpensive and is not affected by toxicity [4,5,10]. Activated carbon (AC) has been used as an effective sorbent to remove pharmaceuticals from contaminated water [12]. The efficiency of AC for removal of various pollutants is related to its high surface area, porosity and versatility [11]. More recently, there is an increasing demand for novel, renewable, locally available and more efficient low-cost materials, for AC production [13]. Coal and lignocellulosic biomass are major sources for the production of commercial activated carbon [14]. The abundance and availability of agricultural by-products make them excellent sources of raw materials for AC production. Some examples of agricultural by-products that have been successfully used in the preparation of AC are coconut shells, wood chips, saw dust, corn cobs, coffee husks, among others [14].

The first aim of this study was to produce two carbonaceous materials from biological secondary sludge and reed weed residues (*Phragmites communis*), and evaluate their characteristics. The second aim was to determine their sorption behavior (kinetics and equilibrium) in batch at different temperatures and pH for SMX removal from aqueous solutions. The pH effects and the thermodynamic

parameters of the systems were discussed in relation with sorption mechanisms of SMX on the materials.

2. Material and methods

2.1. Sorbate

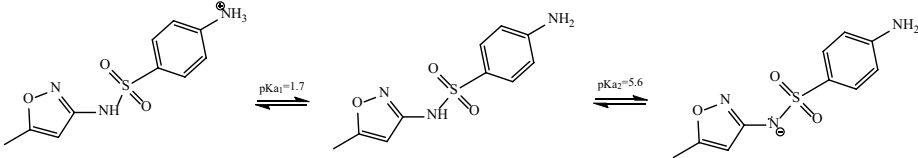
Sulfamethoxazole (SMX) of industrial grade was used as such, without any further purification. SMX stock solutions (200 mg L⁻¹) were prepared using methanol as co-solvent because the solubility of SMX was relatively low in pure distilled water. These solutions were prepared at room temperature, in the dark, 24 h before their use [15]. Some physicochemical properties of the antibiotic are presented in Table 1.

The concentrations of SMX in water were measured with a UV-Visible spectrometer (Genesys 10S, USA). The wavelength of measurement was set at 270 nm [16], where the SMX compound exhibits its maximum UV-Vis absorption. The analytical calibration curve built revealed a good linearity ($r^2 > 0.99$) in the range from 0.025 to 10 mg L⁻¹ SMX, in distilled water.

2.2. Preparation of the sorbents

The raw materials were a residual sludge from an industrial wastewater treatment plant (Lerma WWTP, Mexico), and an herbaceous earthy plant (*Phragmites communis*, from Tenancingo, Mexico). The Lerma WWTP uses a biological activated sludge process and provides treatment to effluents from food industries mainly. The biological sludge and the herbaceous residues were dried at room temperature and then pyrolyzed in a muffle furnace at 550°C for 1 h under nitrogen flow rate of 250 mL min⁻¹. The pyrolyzed solids were milled and sieved. The 0.42–0.84 mm particles fraction was retained and sucked in an acid solution (18% HCl) for 24 h, to remove the ashes, followed by thorough washing with distilled water until reaching a final constant pH. A low sorption capacity resulted from the above-mentioned preparation technique. Consequently, it was modified in a second step. The washed materials were subjected to an additional thermal treatment; this consisted in heating the samples at 800°C, for 1 h more, in a horizontal tubular furnace (Prendo HT3-1100), which improved the sorption capacity. During the 800°C treatment, the environment was not airtight; however, due to limitations on the quantity of air present,

Table 1
Physicochemical properties of sulfamethoxazole (SMX)

Size ^a (Å)	Chemical structure	MW ^b (g mol ⁻¹)	pK _a ^c
12.26		253.28	$pK_{a1} = 1.7$ $pK_{a2} = 5.6$

^aSource: From the study by Chen et al. [41].

^bSource: From the study by Tonucci et al. [16].

^cK_a: acidity constant [41].

only a little part of the carbon was potentially affected by the oxidation reactions. Finally, the produced carbonaceous materials were dried at 100°C for 24 h, and preserved at room temperature in glass containers for later use. The sorbents were identified as SSCM and RCM (secondary sludge carbonaceous material and reed carbonaceous material).

2.3. Sorbent characterization

The SSCM and RCM materials were submitted to the following characterization procedures.

2.3.1. Scanning electron microscopy

Before the SMX sorption tests, the materials were mounted directly on holders and then observed at 10 kV with a scanning electron microscope (JEOL JSM-5900-LD, Japan). Concurrently, microanalysis of the elemental components was carried out by energy X-ray dispersive spectroscopy (EDS probe), at different areas of the samples, at 500X for each material.

2.3.2. Thermogravimetric analysis

A sample in the range of 1–100 mg was placed in the balance of the thermogravimetric analyzer (TGA 51, TA Instrument, New Castle, USA). The TGA was operated in a nitrogen atmosphere with a heating program from 20°C to 800°C at a rate of 10°C min⁻¹.

2.3.3. Point of zero charge (pH_{pzc}), concentrations of the acid–base groups and pH of the carbonaceous materials

At the pH_{pzc} point, there is no charge at the surface of the materials; that is, the total positive charge is equal to the total negative charge [17]. To determine this parameter, a sample of sorbents (10 mg) were placed in opaque vials with a 0.01 M NaCl solution. The NaCl solution was previously adjusted at different pH between 1 and 12 (1 unit interval) with 0.1 M HCl or NaOH solutions. After 24 h of contact, the samples were centrifuged and decanted, and pH was determined in the liquid phases with a potentiometer (HI 2550, HANNA, Mexico).

The determination of acid–base groups was performed as follows. 0.2 g of each biomaterial and 25 mL of 0.025 M NaOH or HCl were shaken during 48 h at room temperature. After that the samples were decanted and the excess acid was titrated with 0.1 M NaOH in the presence of phenolphthalein. The superficial acidity was obtained by a similar procedure using 0.1 M HCl as titrant. The experiments were done in duplicate.

Moreover, the pH_{1,2} of the materials was determined (2 mL of distilled water for 1 g of biomaterial). The test tubes were shaken for 24 h, after which, the samples were centrifuged and decanted before measuring the pH_{1,2} of the liquid phase. The experiments were done in duplicate.

2.3.4. Specific surface area and pore size

The BET (Brunauer–Emmett–Teller) surface area was determined by standard multipoint techniques of nitrogen

sorption using a BELSORP instrument (Japan). Samples of each biomaterial (19 mg) were heated at 373 K for 2 h before the specific surface area was measured.

2.3.5. Fourier transform infrared spectroscopy

Before and after sorption of SMX, the IR spectra of the sorbents were obtained at room temperature in the wavelength range from 4,000 to 400 cm⁻¹ using a Fourier transform infrared spectrometer (Tensor 27 model, Bruker, MA, USA).

2.4. Sorption studies

2.4.1. Kinetic studies

The kinetics of removal of SMX by the SSCM and RCM was studied as follows. 0.01 g of biomaterial and 10 mL aliquot of a SMX solution (10 mg L⁻¹, pH 7) were placed in centrifuge tubes and shaken at 120 rpm, for different times (5, 15, and 30 min, 1, 3, 5, 7, 12, 18, 24, 48, and 72 h). At the end, the samples were centrifuged and decanted. The experiments were done in triplicate. The SMX concentrations were determined in the liquid phases as described above.

The experimental data were fitted to different kinetic models, by non-linear regressions (Origin Pro software 8.1). The evaluated models (Eqs. (1)–(4)) were pseudo-first-order (Lagergren), pseudo-second-order (Ho and McKay), second-order (Elovich) and intra-particle diffusion models [6,18,19]:

$$q_t = q_e(1 - e^{-k_t t}) \quad (1)$$

$$q_t = \frac{1}{b} \ln(1 + abt) \quad (2)$$

$$q_t = \frac{q_e^2 kt}{1 + q_e kt} \quad (3)$$

$$q_t = k_{id} t^{1/2} + C \quad (4)$$

where q_t and q_e (mg g⁻¹) are the adsorbed amount at time t and at equilibrium, respectively; K_t (h⁻¹) is the kinetic constant of Lagergren; a , is the initial sorption rate (mg g⁻¹ h⁻¹) and b is the desorption constant of the Elovich equation (g mg⁻¹); k_t is the pseudo-second-order rate constant (g mg⁻¹ h⁻¹) and k_{id} (mg g⁻¹ h^{-1/2}) is the intra-particle diffusion rate coefficient and C is a constant related to the thickness of the boundary layer.

2.4.2. Sorption isotherms

The equilibrium of the sorption was studied by putting in contact 0.01 g of biomaterial with 10 mL of SMX solutions at different initial concentrations (1–200 mg L⁻¹). The contacting vials were shaken by tumbling, at 120 rpm for 72 h at the end of which the samples were centrifuged and decanted. Then, the equilibrium SMX concentration (C_e , mg L⁻¹) was measured in the liquid phase of each vial and the corresponding sorption capacity (q_e , mg g⁻¹) was determined by mass balance (Eq. (5)).

$$q_e = \frac{(C_0 - C_e)}{w} \times V \quad (5)$$

C_0 (mg L⁻¹) is the initial liquid phase SMX concentration, V (L) is the volume of the liquid and w (g) is the mass of sorbent.

The experimental data were fit with Langmuir, Freundlich and Langmuir–Freundlich isotherm models (Eqs. (6)–(8)) [19–21].

$$q_e = \frac{Q_{\max} K_L C_e}{1 + K_L C_e} \quad (6)$$

$$q_e = K_F C_e^{1/n} \quad (7)$$

$$q_e = \frac{K C_e^{1/n}}{1 + b C_e^{1/n}} \quad (8)$$

where Q_{\max} (mg g⁻¹) is the maximum sorption capacity of SMX per unit weight of sorbent, and K_L (L mg⁻¹) is the Langmuir constant related to the energy of sorption; K_F (mg g⁻¹) (L mg⁻¹)^{1/n} is the Freundlich constant and $1/n$ (dimensionless) is the exponent, which is indicative of the heterogeneity of the surface of the sorbent; and K and b are empirical constants in Eq. (8).

The separation factor, R_L (Eq. (9)) (dimensionless), was calculated from K_L and used to evaluate if the sorption was favorable ($0 < R_L < 1$), unfavorable ($R_L > 1$), linear ($R_L = 1$) or irreversible ($R_L = 0$) [22].

$$R_L = \frac{1}{1 + K_L C_0} \quad (9)$$

2.4.3. Effect of temperature

The thermodynamic parameters are important since they provide relevant information about the sorption processes of the system. The parameters allow knowing the spontaneity of the phenomenon, whether it needs or releases energy and whether the process is reversible or not. Such information can be known from thermodynamic

parameters, namely the Gibb's free energy (ΔG° , kJ mol⁻¹), enthalpy change (ΔH° , kJ mol⁻¹) and entropy change (ΔS° , kJ mol⁻¹ K⁻¹), which can be determined from Eqs. (10) and (11) [11]:

$$\ln\left(\frac{q_e}{C_e}\right) = \frac{\Delta G^\circ}{RT} = -\frac{\Delta H^\circ}{RT} + \frac{\Delta S^\circ}{R} \quad (10)$$

$$\Delta G^\circ = \Delta H^\circ - T\Delta S^\circ \quad (11)$$

where R is the universal gas constant (8.3145 J mol⁻¹ K⁻¹) and T is the temperature in K.

Eq. (10) was applied on the initial concentration range from 1 to 70 mg L⁻¹ and 1 to 100 mg L⁻¹, for SSCM–SMX and RCM–SMX, respectively. Additional sorption equilibrium tests were carried at 303, 313 and 323 K, adding to, and as in the previous isotherm tests (293 K).

2.4.4. Effect of pH

Batch equilibrium tests were carried out by putting in contact 0.01 g of biomaterial with 10 mL aliquots of 10 mg L⁻¹ SMX solution. The pH values of the solutions were adjusted at different levels from 2 to 12. The solutions were shaken for 72 h. At the end, the samples were centrifuged and decanted. Then, the pH and SMX equilibrium concentration was measured in the liquid phase. Experiments were performed in triplicate.

3. Results and discussion

3.1. Scanning electron microscopy

The scanning electron microscopy (SEM) micrographs of the materials (SSCM and RCM), before sorption, are shown in Fig. 1. The SSCM carbon had irregular flake-shaped aggregates of 10–100 μm diameters. Similar observations have been reported elsewhere [18]. Meanwhile, the image of the RCM solids showed a carbonized cellular structure composed by a subset of tubes, which were the channels through which nutrients were transported to the rest of the plant [23]. The thermic and acid treatment favored

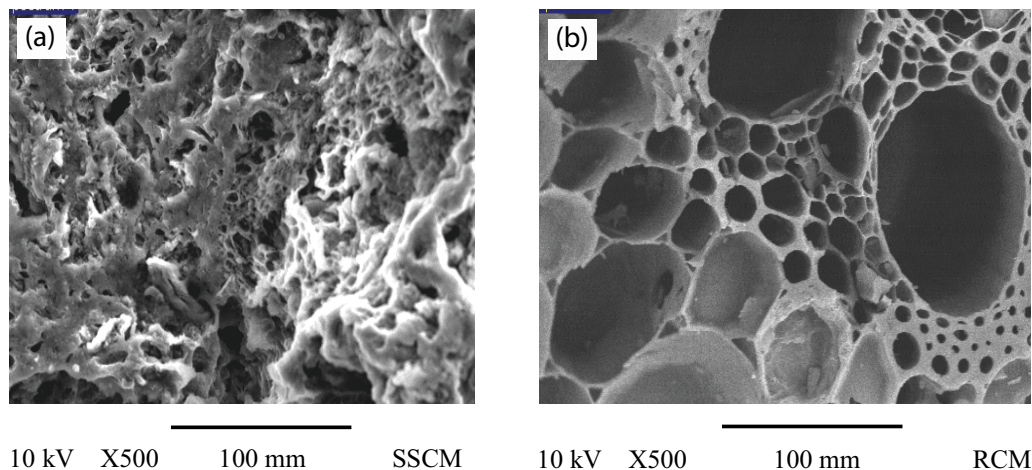


Fig. 1. Scanning electron microscopy (SEM) images of (a) SSCM and (b) RCM before sulfamethoxazole sorption.

the decomposition of the organic matter in the carbons, resulting in fluffy materials with high porosity. In this study, acid-wash treatment was able to remove most of the inorganic fractions from the carbonaceous materials.

Table 2 shows the elemental composition of both materials before the SMX sorption, after each of the treatments steps (pyrolysis at 500°C, acid wash, additional heating at 800°C). Basic elements found for SSCM were C, O, Si, Al and Ca. Other authors have detected the same components for their carbonaceous material derived from biological secondary sludge also [18,24]. The presence of Al, K, Fe, Na, Ti and Mo is attributed to the composition of the raw material (waste activated sludge from industrial wastewater). The C content of the sorbents was relatively stable across the increasing pyrolytic temperatures and with the thermic and the acid treatments, whereas the O content increased, and the N content decreased.

Acidic modification of materials can introduce major changes into their physico-chemical properties. For example, the O/C ratio increased by using pyrolysis, thermic, and then acid treatment, compared with only pyrolysis, which indicates that the surface polar functional groups could be increased.

The acid treatment generally decreased the Ca, K, Mg and Fe contents of the SSCM material. The final RCM sorbent had only three elements, C, O, and a little amount of Si. The C content of the RCM was up to 87%, as expected for cellulosic materials [19] while Si was probably from the nutrients taken up by plants from the soil [23]. The O/C ratio also increased using pyrolysis, thermic and then an acid treatment, which indicates that the materials had a more oxidized surface, which influences the π - π electron-donor/acceptor interactions. This behavior is opposite in other studies, where the O/C atomic ratios were decreasing with increasing pyrolytic temperatures [25,26].

Nitrogen was present in the pyrolyzed and acid-washed carbons, but completely disappeared after the final thermic treatment (800°C). The loss of nitrogen in both materials was attributed to its volatilization during the pyrolysis [25] and thermic treatment (800°C).

3.2. Physicochemical properties of the sorbents

Table 3 shows the main physicochemical characteristics of the materials such as $pH_{1,2}$, pH_{pZC} , and acid and base group concentrations, S_{BET} , total pore volume and pore size. The $pH_{1,2}$ values of the materials SSCM and RCM were 6.6 and 7.0, respectively, indicating that both materials nearly had a neutral character. The initial pH of the solutions of SMX was 6.0 and the pH of SMX equilibrium concentration, 7.0 and 7.2, for SSCM and for RCM, respectively.

The pH_{pZC} values for SSCM and RCM were 7.1 and 7.3, respectively, which indicate that both materials will have a positive net surface charge up to pH_{pZC} . Therefore at pH values lower than the zero point charge of the sorbents, the SMX^- may be attracted, while it will be repelled at higher pH values.

Concerning the acid and base group concentrations (H^+ and OH^- on Table 3), the former were slightly higher than the latter on the surface of the sorbents, which provides a net positive charge depending on the pH of the solutions, compared with pH_{pZC} . In surface of reed biochar, charges were negative at pH 7, caused by deprotonation of the oxygen-containing functional groups such as carboxyl and hydroxyl groups [27].

The specific surfaces were fairly high (S_{BET} of 266 and 631 $m^2 g^{-1}$ for SSCM and RCM, respectively). Based on the mean pore size, it was determined that SSCM and RCM were meso- and microporous, respectively. The RCM pore size was smaller, but its overall volume was higher, compared

Table 2
EDS analysis of SSCM and RCM before sulfamethoxazole sorption

Element	SSCM 500°C	SSCM 500°C + HCl	SSCM 500°C + HCl + 800°C	RCM 500°C	RCM 500°C + HCl	RCM 500°C + HCl + 800°C
Percentages weight (%)						
C	77.1 ± 0.5	70.4 ± 8.7	72.3 ± 1.3	83.7 ± 7.4	84.1 ± 12.8	87.2 ± 8.2
N	11.5 ± 0.9	ND	ND	13.2	16.7 ± 0.8	ND
O	9.6 ± 5.1	12.7 ± 5.4	20.0 ± 1.2	6.5 ± 0.76	5.7 ± 0.2	12.0 ± 7.3
Si	2.1 ± 0.3	11.7 ± 2.5	5.9 ± 0.4	ND	0.24	0.9 ± 0.8
Ca	ND	0.6 ± 0.1	0.4 ± 0.1	ND	ND	0.4
S	ND	2.0 ± 0.4	ND	0.3 ± 0.1	0.14	ND
Cl	ND	0.7 ± 0.2	ND	0.8 ± 0.1	0.4 ± 0.09	ND
Al	ND	0.8 ± 0.2	0.7 ± 0.2	ND	ND	ND
Mg	0.11	ND	ND	0.17	ND	ND
K	ND	0.3 ± 0.03	0.12	4.2 ± 0.4	ND	ND
Fe	ND	0.5 ± 0.1	0.2	ND	ND	ND
Na	ND	ND	0.3	ND	ND	ND
Ti	ND	0.4 ± 0.007	0.2 ± 0.1	ND	ND	ND
Mo	ND	ND	0.2 ± 0.1	ND	ND	ND

ND: Not detected.

Table 3
Physicochemical properties of the sorbents

Material	SSCM	RCM
pH _{1:2}	6.6	7.0
pH _{PZC}	7.1	7.3
H ⁺ meq g ⁻¹	172	153
OH ⁻ meq g ⁻¹	130	135
S _{BET} (m ² g ⁻¹)	266.18	631.76
Total pore volume (cm ³ g ⁻¹)	0.2976	0.3518
Mean pore size (Å)	44.7	22.3

with SSCM. Comparable results were observed between two sorbents which were derived from sewage and waste oil sludges [2]. The study of three pine-wood biochars prepared under different thermochemical conditions, such as pyrolysis at 400°C and 500°C and pyrolysis carried out at 500°C followed by hydrogenation, showed that the surface area and pore volume increased significantly with the pyrolytic temperature [15]. This indicates that the pyrolysis conditions might play a role in the sorption capacities. Also, according to Tables 1 and 3, the molecular size of SMX is favorable for its sorption in the pores of both materials.

3.3. Thermogravimetric analysis

Pyrolytic characteristics of the materials were examined by the TGA technique. Three stages of mass loss were observed (figure not shown). In the first stage, the mass loss of RCM was less significant than for SSCM. The weight loss of the materials mainly occurs in the range of ~30°C to 100°C, corresponding to 5.2% and 1.3% of the initial masses of SSCM and RCM, respectively, which was attributed to the dehydration process. In the second stage, the weight loss occurs between 100°C and 800°C (1.6% and 0.9%, for SSCM and RCM, respectively), corresponding to degradation of hemicellulose, organic and/or aqueous extractives, cellulose and lignin, according to the study by Suárez-García et al. [28]. In the third stage, weight lost above 800°C was 10% and

5%, for SSCM and RCM. The data confirm the high thermal stability of both materials in the range of 100°C–800°C.

3.4. Fourier transform infrared spectroscopy

The surface functional groups of the materials before and after SMX sorption were characterized using Fourier transform infrared spectroscopy (FT-IR) analysis. The corresponding results are presented in Fig. 2. The spectra show differences in chemical composition due to the nature and origin of the materials. All bands assignments from the FT-IR spectra indicated that both materials contained the following groups on its surface: –OH, –COOH and C=C. Therefore, π - π and H-bonding interactions should be considered to evaluate the sorption of SMX from aqueous solution by materials.

Before SMX sorption (Fig. 2a, black line), the SSCM spectra showed the following bands: at 2,944 and 2,900 cm⁻¹, which are associated with the C–H stretching vibration; at 2,677 cm⁻¹, corresponding to the C–H stretching vibration of the aromatic groups; at 1,571 and 1,541 cm⁻¹ due to the C=C groups; at 1,106 and 468 cm⁻¹, for the C=O and C–C=O groups [29,30]. After SMX sorption on the SSCM material (red line), the intensities of the bands at 2,617, 2,081, 1,106 and 468 cm⁻¹ were reduced, which confirm that the SMX molecules were present in the surface of the material.

The bands of the RCM spectra, before SMX sorption (Fig. 2b, black line), were at 3,014, 2,699 and 1,096 cm⁻¹ corresponding to OH stretching vibration, aromatic groups and C–O stretching vibration associated to cellulose chains [23]. More bands were at 792 and 466 cm⁻¹, which correspond to the vibrations of the C=C and C–C=O groups [29,30]. The RCM spectra after SMX sorption (red line) showed a decrease of the intensity of the bands at 1,096 and 466 cm⁻¹ and the apparition of some new bands at around 3,043, 3,014 and 2,875 cm⁻¹, corresponding to the vibration of C–H groups in the aromatic compound (SMX). The bands at 2,113 cm⁻¹ correspond to the NH groups.

The surface functional groups of the materials containing oxygen participate in the SMX sorption. Another study found that acid treatments for 24 and 48 h greatly affect the

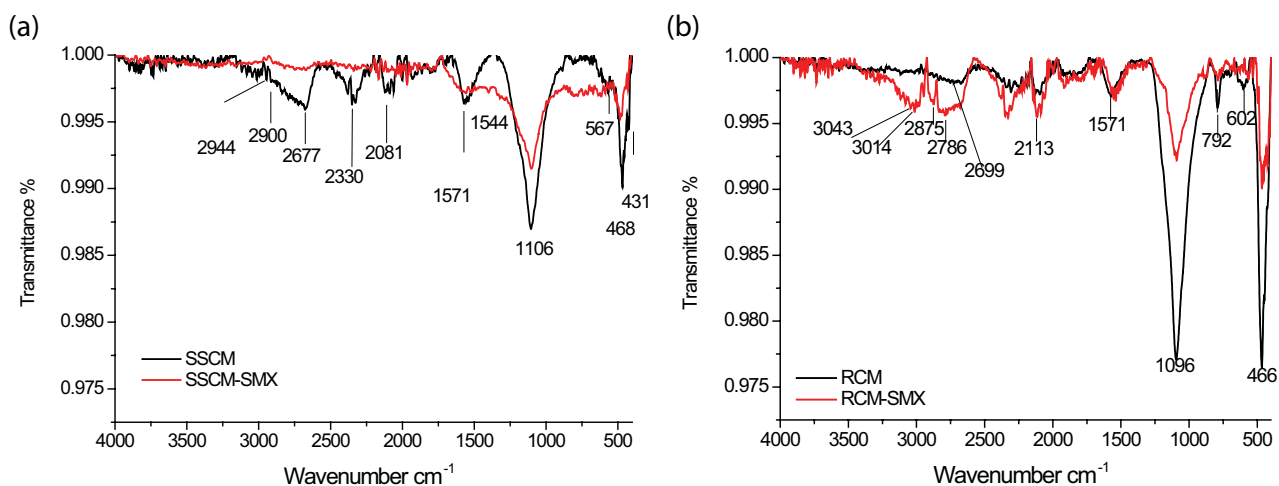


Fig. 2. FT-IR spectrum of SSCM (a) and RCM (b), before (black line) and after (red line) sulfamethoxazole sorption.

sorption capacity of activated carbon. FT-IR spectra have revealed that longer exposure time did not produce more oxygen containing functional groups at the surface of the sorbent; it rather cut the functionalization due to water cluster formation effect. These acidic groups block the reactive sorption sites and ultimately reduce the sorption capacity [31]. On the other hand, moderate exposure time encouraged the oxygen-containing functional groups to attach on the surface of activated carbon and improved the surface chemistry of modified activated carbon. Other authors explain that the acid treatment breaks the pore wall and expands microspores into meso- or macropores [32].

3.5. Sorption experiments

3.5.1. Kinetic studies

Kinetic studies were used to determine the equilibrium time for the sorption process and to understand the removal mechanism involved in the sorption of SMX by the materials. The removal mechanisms are often governed by the interactions of organic pollutants with various attributes of the biochar, primarily via chemisorption (electrophilic interaction) and physisorption through COOH, OH and R-OH functional groups [33].

Fig. 3 shows the relationship between contact time and sorption capacities of the materials. The parameters of the kinetic models are given in Table 4, for the pseudo-first-order, second-order, and pseudo-second-order models. According to Fig. 3, the adsorbed amounts increased quickly in the first 5 h and then slowly in the rest of time. This kind of behavior is common to sorption of great organic molecules [34]. In both cases (SSCM and RCM), a perfectly defined plateau was not observed. However, for practical proposes, it was considered that the sorption process reached a pseudo-equilibrium state at 72 h, because after this time the sorption capacity does not show a considerable increase. According to the correlation coefficients (R^2), the kinetic data were best fitted by the second-order equation (Elovich model), for both materials

(Table 4). This suggests that chemisorption could be one of the probable mechanisms of SMX sorption on the surface of the materials. Moreover, it was observed that the adsorption and desorption rates parameters (a and b) were similar for SSCM and RCM. Ahmed et al. [35] also reported that the pseudo-second-order kinetic model was the most suitable rate law for describing the sorption of a mixture of sulfonamides (sulfamethazine, sulfamethoxazole and sulfathiazole) and chloramphenicol onto functionalized biochar. During the sorption of sulfamethazine on straw biochars pyrolyzed at 300°C and 600°C; the physisorption (partition) and weak chemical binding (π - π EDA interaction) could be the dominating sorption processes, respectively [36].

As shown in Table 4, using the intra-particle diffusion model in its original form (Eq. (4)) did not allow to fit the data (low R^2). However, when this model was modified by considering that the intra-particle diffusion (Fig. 4, q_t as a function of $t^{1/2}$) occurs in two or three steps at different rates (K_1 , K_2 and K_3), the quality of the fit improved, yielding adequate R^2 values, at least for the first two steps (Table 4). This means that, apparently, intra-particle diffusion could be one of the significant mechanisms that were limiting the rate of the SMX sorption onto both SSCM and RCM. Moreover, it can be observed in Fig. 4 that lines for the first intra-particle diffusion steps do not pass at the origin; the C_1 constants (Eq. (4)) were above zero, which indicates the coexistence of other limiting mechanisms such as external film diffusion, together with intra-particle diffusion. The C_1 constant was found to vary proportionally to the boundary layer thickness [19].

Overall, the multi-steps intra-particle diffusion model can be interpreted as it follows. At the beginning, after passing the surrounding liquid boundary layer, the sorbate becomes attached at the outer surface of the particles, at a very fast rate. When sorption at the external surface reached saturation, the sorbate entered into the pores of the sorbent particle, which increased the resistance of the diffusion process and decreased the diffusion rates [37].

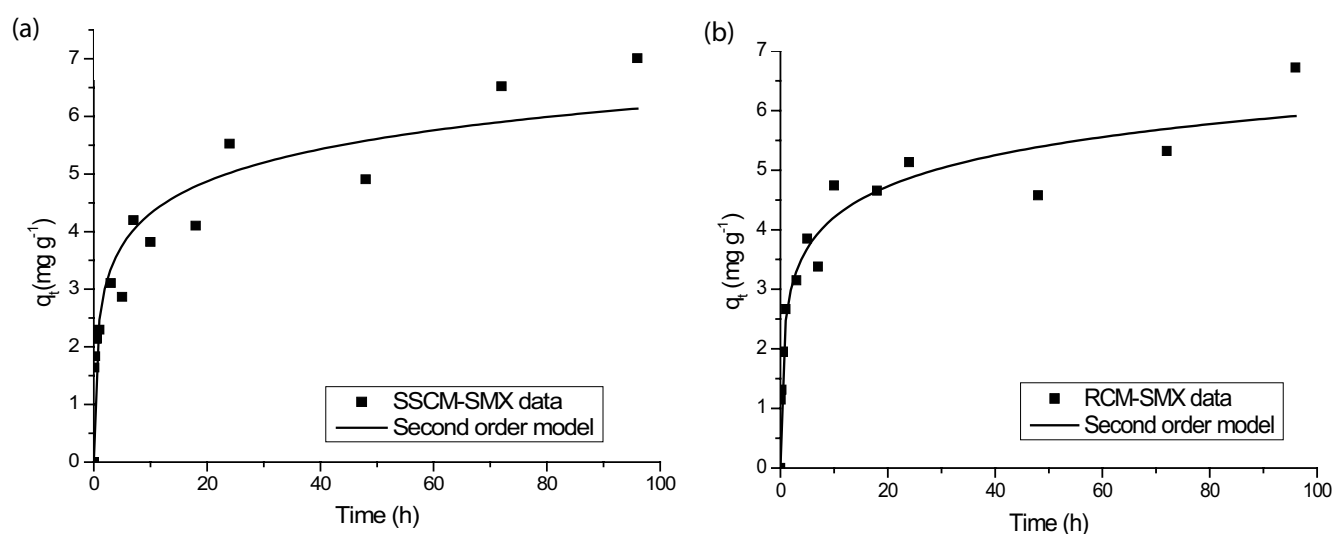


Fig. 3. Sorption kinetics of SMX by SSCM (a) and RCM (b), with adjustment to second-order model.

Table 4
Kinetic parameters of SMX sorption by SSCM and RCM

Model	Parameters	Material	
		SSCM	RCM
Pseudo-first-order	q_e (mg g ⁻¹)	5.53	4.85
	K_L (h ⁻¹)	0.20	0.54
	R^2	0.659	0.784
Pseudo-second-order	q_e (mg g ⁻¹)	5.83	5.25
	k (g mg ⁻¹ h ⁻¹)	0.06	0.14
	R^2	0.757	0.870
Second-order	a (mg g ⁻¹ h ⁻¹)	16.84	19.94
	b (g mg ⁻¹)	1.23	1.32
	R^2	0.907	0.945
Intra-particle diffusion (One step)	K (mg g ⁻¹ h ^{1/2})	0.53	0.65
	C (mg g ⁻¹)	1.90	1.70
	R^2	0.9174	0.8194
(Multi-steps) Stage 1	K_1 (mg g ⁻¹ h ^{1/2})	1.00 ($R^2 = 0.9896$)	2.23 ($R^2 = 0.9457$)
	C_1 (mg g ⁻¹)	1.35	0.37
Stage 2	K_2 (mg g ⁻¹ h ^{1/2})	0.46 ($R^2 = 0.8628$)	0.84 ($R^2 = 0.7206$)
	C_2 (mg g ⁻¹)	2.37	1.74
Stage 3	K_3 (mg g ⁻¹ h ^{1/2})	–	0.11 ($R^2 = 0.5875$)
	C_3 (mg g ⁻¹)	–	4.35

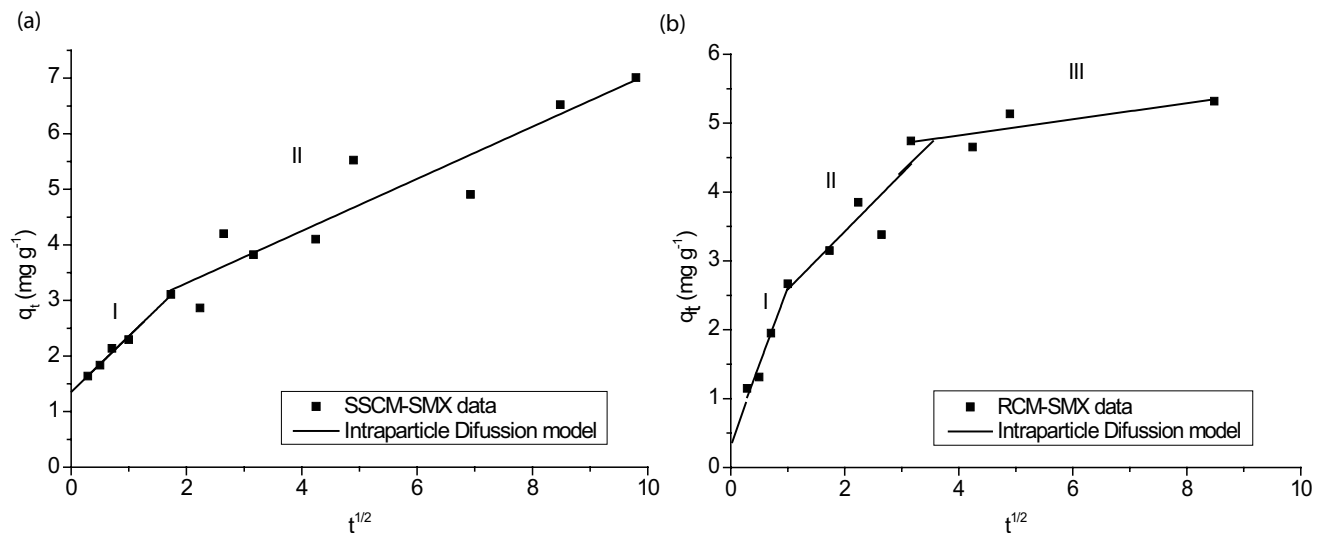


Fig. 4. Multi-steps intra-particle diffusion model for (a) SSCM-SMX and (b) RCM-SMX.

3.5.2. Sorption isotherms

The sorption isotherms of SMX onto the materials at room temperature are shown in Fig. 5. In this figure, it can be seen that the sorption of SMX is higher for SSCM than for RCM in the same experimental conditions. The isotherm shape (concavity) provides important information about how favorable the sorption process is [16]. In this case, both systems exhibited downward concavity.

The sorption equilibrium data were fitted with Langmuir, Freundlich and Langmuir–Freundlich isotherm models. The parameters obtained from the Langmuir model (Table 5) show that the maximum sorption capacities were 30.4 and 21.5 mg g⁻¹ for SSCM and RCM, respectively. For the SSCM material, the Freundlich model fitted very well the isotherm data, better than the Langmuir and Langmuir–Freundlich models. The Freundlich model indicates the heterogeneity of the sorbent surface and considers a multilayer sorption

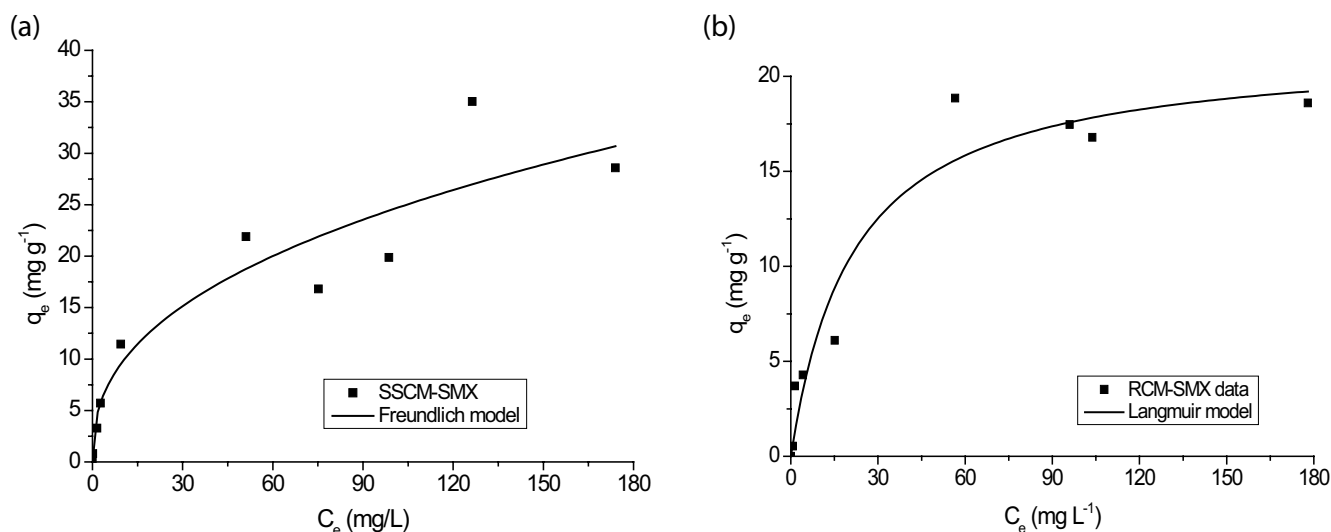


Fig. 5. Sorption isotherms of SMX by SSCM (a) and RCM (b) (72 h contact time at pH 6.0 and room temperature).

Table 5
Isotherm parameters for SMX sorption by SSCM and RCM

Model	Parameters	Material	
		SSCM	RCM
Langmuir	Q_{\max} (mg g ⁻¹)	30.43	21.53
	K_L (L mg ⁻¹)	0.04	0.04
	R^2	0.856	0.942
Freundlich	K_F (mg g ⁻¹) (L mg ⁻¹) ^{1/n}	3.86	2.98
	1/n	0.40	0.37
	R^2	0.888	0.905
Langmuir–Freundlich	K	3.81	1.12
	1/n	0.41	0.95
	B	0.09	0.05
	R^2	0.872	0.934

phenomenon [22]. The values of $1/n$ in the Freundlich model of SSCM and RCM were 0.40 and 0.37, respectively, suggesting that the surface of the sorbents is very heterogeneous [24]. This is in agreement with another study on SMX sorption with biochars derived from anaerobically digested bagasse [10]. Furthermore, in a study of various graphene-based materials and multi-walled carbon nanotubes for sulfamethoxazole sorption, the Freundlich model appeared to be slightly better than the Langmuir model [38].

For the RCM, the best fit isotherm model was the Langmuir model, compared with the Freundlich and Langmuir–Freundlich models. The Langmuir isotherm assumes that the adsorption is limited to a monolayer on the homogeneous surface of the sorbent, where the binding sites possess the same capacity without any interaction between them [24]. The parameter K_L was of the same order of magnitude for both materials. Other authors studied SMX sorption on carbonaceous materials, and also observed that the Langmuir and Langmuir–Freundlich models were most

appropriate. Furthermore, in the present study, the parameter R_L (using C_0 from 1 to 200 mg L⁻¹) was calculated for the SMX, being the values between 0.958 and 0.093 and 0.960 to 0.097, for SSCM and RCM, respectively, indicating that the sorption process was favorable [8,16].

Table 6 shows the sorption capacities of sulfamethoxazole by different waste-derived carbonaceous materials (single-compound aqueous solutions). For instance, [8] studied SMX sorption on various carbonaceous materials from waste. Their sorption capacity values were between 4 and 7 mg g⁻¹, which are well below those reported in this work. In contrast, Tonucci et al. [16] studied several activated carbons (from pine, coconut shell and mineral carbon), reaching the maximum sorption capacities of 58–130 mg g⁻¹, which were higher than the values found in the present study.

3.5.3. Temperature effects on adsorption equilibrium

The influence of temperature (T) was studied at 303, 313 and 323 K, at different concentrations (Fig. 6). ΔH° and ΔS° were obtained from Eq. (10), from the slope and intercept, respectively, of the linear plot of $\ln(q/C_e)$ vs. $1/T$. ΔG° was then calculated with Eq. (11). The thermodynamic parameters obtained are summarized in Table 7.

For both materials (SSCM and RCM), the ΔG° values were negative, which indicates that the SMX removal process is spontaneous and favorable. The magnitude of the absolute values increased with T , which indicates that at 323 K, the spontaneity of the removal process increases, since the driving force of the adsorption process is higher in both carbonaceous materials [12,21]. By considering the previous criterion to compare the materials, the RCM system presents a greater motive power than SSCM (Table 7). In the literature, the magnitude of the ΔG° value is often used to differentiate between physical and chemical sorption. Lian et al. [21] consider the range from -20 to 0 kJ mol⁻¹ as physisorption, compared with -400 to -800 kJ mol⁻¹ for chemisorption. Based on the aforementioned criterion, the dominant mechanism was physisorption for both systems in this study

Table 6
Comparison of sorption capacities for SMX by some sorbents

Sorbent	Q_{\max} (mg g ⁻¹)	Reference
Fish waste	1.31	[8]
Sewage sludge	7.01	[8]
Carbon nanotubes	30.58	[16]
Mineral carbon	58.35	[16]
Powered activated carbon (Pinus tree)	130.73	[16]
Functionalized biochar	34.01	[32]
Graphene oxide	12.00	[20]
Biochar derived from rice straw	1.82	[42]
Wakefield biochar	21.7	[43]
Reduced graphene oxide (rGO)	11.76	[44]
SSCM	30.43	This work
RCM	21.53	This work

(SSCM–SMX and RCM–SMX). However, by considering the AG data as the barrier between the two mechanisms, the adsorption in the RCM system could also be chemically driven.

Concerning the ΔH parameter, for both materials the values were also negative, indicating that the sorption process was exothermic. For the enthalpy parameter, Çalişkan and Gökürk [12] suggest the following limits to differentiate between physisorption (absolute ΔH value less than 84 kJ mol⁻¹) and chemisorption (ΔH from 84 to 420 kJ mol⁻¹). Based on this criterion, both sorption systems were physically driven. In addition, the magnitude of the enthalpy values obtained for the materials (Table 7) are typical to the hydrogen bond sorption strength (2–40 kJ mol⁻¹) [39]; this suggest that hydrogen bonding interaction has a dominant role in the SMX sorption process.

Finally, for the entropy (ΔS°), positive values were obtained, which indicates that the removal of the adsorbed

SMX can be reversible [11,39]. By comparing the ΔS° parameters (0.03 kJ mol⁻¹ K⁻¹ for SSCM vs. 0.07 kJ mol⁻¹ K⁻¹ for RCM), it is evident that the value of the RCM is higher, which indicates a more ordered arrangement of the SMX molecules on the RCM surface [12].

3.5.4. Mechanisms of the pH effects on the sorption

The pH of the solution is an important parameter that may control the sorption capacity of organic compounds onto sorbents; it affects not only the surface charge of the materials but also the degree of ionization and speciation of the SMX molecules [7]. Fig. 7 reports the variation of the SMX sorption capacities (at $C_0 = 10$ mg L⁻¹) as a function of pH (2–12) of the solution, for the SSCM and RCM. It is evident that the amount of SMX adsorbed by the carbons depends on the pH. Both materials showed a higher removal capacity in acidic conditions and a significantly lower sorption capacity with increasing pH. In general, the increased pH results in increased ionization, solubility and hydrophilicity of the ionizable organic chemicals, and consequently, in a decrease of the sorption. At pH 2, the SMX solution is dominated by both protonated and neutral

Table 7
Thermodynamic parameters of the SSCM–SMX and RCM–SMX systems

Biomaterial	T (K)	Thermodynamic parameters		
		ΔG° (kJ mol ⁻¹)	ΔH° (kJ mol ⁻¹)	ΔS° (kJ mol ⁻¹ K ⁻¹)
SSCM	303	-19.03		
	313	-19.38	-8.42	0.03
	323	-19.73		
RCM	303	-46.78		
	313	-47.46	-26.10	0.07
	323	-48.14		

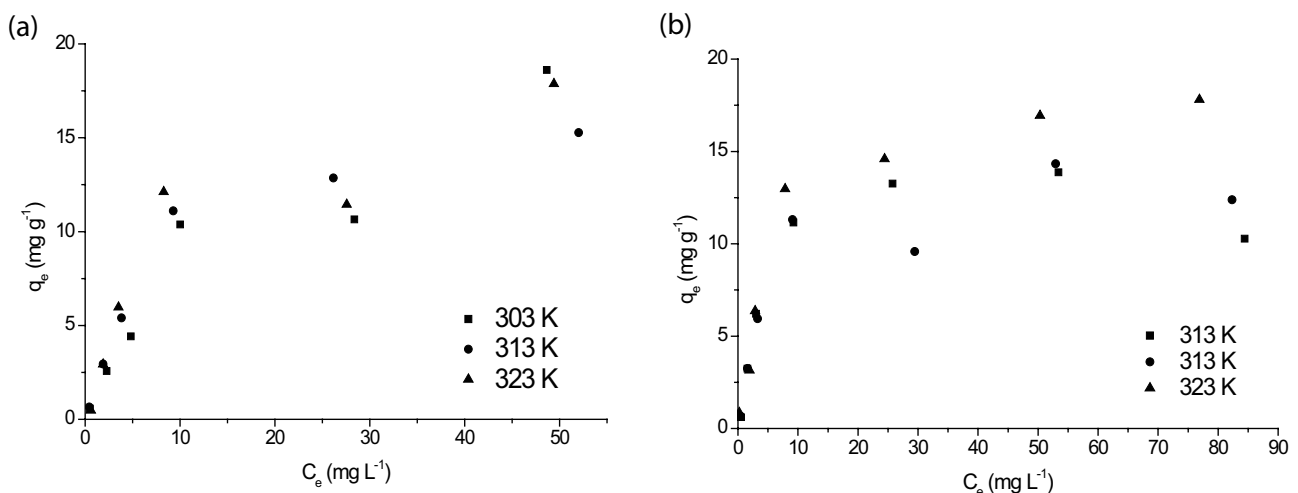


Fig. 6. Sorption isotherms of sulfamethoxazole by SSCM (a) and RCM (b) at different temperatures, where $T =$ (■) 303 K; (●) 313 K; (▲) 323 K.

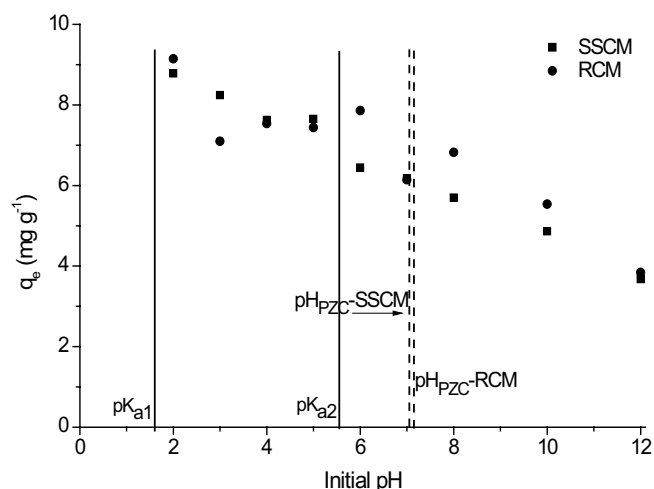


Fig. 7. Effect of pH on sulfamethoxazole by SSCM and RCM. Vertical dark lines represent the two pK_a values of sulfamethoxazole and the dotted lines represent the pH_{PZC} of SSCM and RCM.

species [40], and the surface becomes positively charged as a result, which is the state in which these materials reach their highest sorption capacity. The protonated species is an even stronger π -electron acceptor than the neutral species due to the electron-withdrawing ability of the positively charged amino group [15].

At pH 2–4, the predominant species are the neutral SMX, with which the protonation could facilitate a strong π - π electron donor-acceptor interaction, between the SMX and the materials. At pH 5.6, the SMX solution is dominated by both neutral and negatively charged species (50:50); the π - π EDA interactions are still available between neutral SMX and the carbonaceous surfaces. Since neutral SMX could be the only species present in the solution, SMX sorption slightly decreased.

At pH above 7, stronger Lewis acid base interactions can occur between the basic groups of sulfonamides and the aromatic carboxyl and hydroxyl groups of the carbonaceous surface [35].

At pH 7.3, the net charge at the surface of the materials is zero; both the positive and negative charges are present in same quantities (50% at equilibrium). Furthermore, the negative SMX is the predominant species, so SMX sorption slightly decreases. At higher pH, all the SMX molecules as well as the surface of the materials are negatively charged, generating a strong electrostatic repulsion [20]; therefore, the sorption of the SMX is reduced. A similar trend of the pH effects was observed for the removal of sulfamethoxazole and sulfapyridine by different biochars [10] and of sulfonamides by pine wood biochars prepared under different thermochemical conditions [15].

Another possible mechanism of sorption of SMX by the materials could be through hydrogen bonding between the $-COOH$ groups of the sorbent surface and the $-NH_2$, $-NO_2$ or hydrogen groups present in sulfonamides, [35]. The latter mechanism can be demonstrated through the FT-IR/ATR technique (shifted areas of the functional groups of the SMX-sorbent surface).

4. Conclusions

In this work, two carbonaceous materials obtained by pyrolysis from biological secondary sludge (SSCM) and reed terrestrial weed (RCM) were tested for sulfamethoxazole (SMX) sorption from aqueous solution. The chemical treatment of the materials affected the SMX removal behavior. Both materials exhibited an acidic character with an almost neutral pH_{PZC} . The specific surface was higher for RCM (S_{BET} of $631 \text{ m}^2 \text{ g}^{-1}$) than for SSCM ($266 \text{ m}^2 \text{ g}^{-1}$). The mechanisms responsible for SMX sorption by the activated carbons were comprehensively discussed. Based on the intra-particle diffusion model, it was shown that SMX sorption occurs in several stages (two for SSCM and three for RCM). Concerning the isotherms, the maximum sorption capacities were 30 and 21 mg g^{-1} , for the SSCM and RCM, respectively. According to the thermodynamic parameters, the SMX sorption was spontaneous, favorable, exothermic and reversible. Overall, based on the uptake capacity of the materials produced and the knowledge of their characteristics and their adsorption mechanisms, the waste-derived activated carbons are potentially useful for SMX removal from water.

Acknowledgment

The authors would like to acknowledge financial support from Universidad Autónoma del Estado de México (Grant No. 4523/2018/CI) and CONACYT (Scholarship No. 265605).

References

- [1] S. Álvarez-Torrellas, A. Rodríguez, G. Ovejero, J. García, Comparative adsorption performance of ibuprofen and tetracycline from aqueous solution by carbonaceous materials, *Chem. Eng. J.*, 283 (2016) 936–947.
- [2] R. Ding, P. Zhang, M. Seredych, T.J. Bandoz, Removal of antibiotics from water using sewage sludge- and waste oil sludge-derived adsorbents, *Water Res.*, 46 (2012) 4081–4090.
- [3] A.M.L. Fernández, M. Rendueles, M. Díaz, Competitive retention of sulfamethoxazole (SMX) and sulfamethazine (SMZ) from synthetic solutions in a strong anionic ion exchange resin, *Solvent Extr. Ion Exch.*, 32 (2014) 763–781.
- [4] G.Z. Kyzas, J. Fu, N.K. Lazaridis, D.N. Bikiaris, K.A. Matis, New approaches on the removal of pharmaceuticals from wastewaters with adsorbent materials, *J. Mol. Liq.*, 209 (2015) 87–93.
- [5] Md.A. Ahsan, Md.T. Islam, C. Hernandez, H. Kim, Y. Lin, M.L. Curry, J. Gardea-Torresdey, J.C. Noveron, Adsorptive removal of sulfamethoxazole and bisphenol a from contaminated water using functionalized carbonaceous material derived from tea leaves, *J. Environ. Chem. Eng.*, 6 (2018) 4215–4225.
- [6] R. Rostamian, H. Behnejad, A comparative adsorption study of sulfamethoxazole onto graphene and graphene oxide nanosheets through equilibrium, kinetic and thermodynamic modeling, *Process Saf. Environ. Prot.*, 102 (2016) 20–29.
- [7] M.B. Ahmed, J.L. Zhou, H.H. Ngo, W. Guo, Adsorptive removal of antibiotics from water and wastewater: progress and challenges, *Sci. Total Environ.*, 532 (2015) 112–126.
- [8] L. Nielsen, T.J. Bandoz, Analysis of sulfamethoxazole and trimethoprim adsorption on sewage sludge and fish waste derived adsorbents, *Microporous Mesoporous Mater.*, 220 (2016) 58–72.
- [9] A.J. Watkinson, E.J. Murby, S.D. Costanzo, Removal of antibiotics in conventional and advanced wastewater treatment: implications for environmental discharge and wastewater recycling, *Water Res.*, 41 (2007) 4164–4176.

- [10] Y. Yao, Y. Zhang, B. Gao, R. Chen, F. Wu, Removal of sulfamethoxazole (SMX) and sulfapyridine (SPY) from aqueous solutions by biochars derived from anaerobically digested bagasse, *Environ. Sci. Pollut. Res.*, 25 (2018) 25659–25667.
- [11] G. Moussavi, A. Alahabadi, K. Yaghmaeian, M. Eskandari, Preparation, characterization and adsorption potential of the NH_4Cl -induced activated carbon for the removal of amoxicillin antibiotic from water, *Chem. Eng. J.*, 217 (2013) 119–128.
- [12] E. Çalışkan, S. Göktürk, Adsorption characteristics of sulfamethoxazole and metronidazole on activated carbon, *Sep. Sci. Technol.*, 45 (2010) 244–255.
- [13] M. Momčilović, M. Purenović, A. Bojić, A. Zarubica, M. Randelović, Removal of lead(II) ions from aqueous solutions by adsorption onto pine cone activated carbon, *Desalination*, 276 (2011) 53–59.
- [14] T.M. Alslaibi, I. Abustan, M.A. Ahmad, A.A. Foul, A review: production of activated carbon from agricultural byproducts via conventional and microwave heating, *J. Chem. Technol. Biotechnol.*, 88 (2013) 1183–1190.
- [15] M. Xie, W. Chen, Z. Xu, S. Zheng, D. Zhu, Adsorption of sulfonamides to demineralized pine wood biochars prepared under different thermochemical conditions, *Environ. Pollut.*, 186 (2014) 187–194.
- [16] M.C. Tonucci, L.V.A. Gurgel, S.F. de Aquino, Activated carbons from agricultural byproducts (pine tree and coconut shell), coal, and carbon nanotubes as adsorbents for removal of sulfamethoxazole from spiked aqueous solutions: kinetic and thermodynamic studies, *Ind. Crops Prod.*, 74 (2015) 111–121.
- [17] A. Blanco-Flores, A. Colín-Cruz, E. Gutiérrez-Segura, V. Sánchez-Mendieta, D.A. Solís-Casados, M.A. Garrudo-Guirado, R. Batista-González, Efficient removal of crystal violet dye from aqueous solutions by vitreous tuff mineral, *Environ. Technol. (UK)*, 35 (2014) 1508–1519.
- [18] S. Pinedo-Hernández, E. Gutiérrez-Segura, M. Solache-Ríos, A. Colín-Cruz, Properties of carbonaceous materials from sewage sludge to remove organic matter. Phenol as a particular case, *Desal. Wat. Treat.*, 72 (2017) 126–135.
- [19] E.J. Lara-Vásquez, M. Solache-Ríos, E. Gutiérrez-Segura, Malachite green dye behaviors in the presence of biosorbents from maize (*Zea mays* L.), their Fe-Cu nanoparticles composites and Fe-Cu nanoparticles, *J. Environ. Chem. Eng.*, 4 (2016) 1594–1603.
- [20] S.-W. Nam, C. Jung, H. Li, M. Yu, J.R.V. Flora, L.K. Boateng, N. Her, K.-D. Zoh, Y. Yoon, Adsorption characteristics of diclofenac and sulfamethoxazole to graphene oxide in aqueous solution, *Chemosphere*, 136 (2015) 20–26.
- [21] F. Lian, B. Sun, Z. Song, L. Zhu, X. Qi, B. Xing, Physicochemical properties of herb-residue biochar and its sorption to ionizable antibiotic sulfamethoxazole, *Chem. Eng. J.*, 248 (2014) 128–134.
- [22] A.M. Sevim, R. Hojiyev, A. Gül, M.S. Çelik, An investigation of the kinetics and thermodynamics of the adsorption of a cationic cobalt porphyrine onto sepiolite, *Dyes Pigm.*, 88 (2011) 25–38.
- [23] G. García-Rosales, A. Colín-Cruz, Biosorption of lead by maize (*Zea mays*) stalk sponge, *J. Environ. Manage.*, 91 (2010) 2079–86.
- [24] E. Gutiérrez-Segura, M. Solache-Ríos, A. Colín-Cruz, C. Fall, Adsorption of cadmium by Na and Fe modified zeolitic tuffs and carbonaceous material from pyrolyzed sewage sludge, *J. Environ. Manage.*, 97 (2012) 6–13.
- [25] H. Zheng, Z. Wang, X. Deng, J. Zhao, Y. Luo, J. Novak, S. Herbert, B. Xing, Characteristics and nutrient values of biochars produced from giant reed at different temperatures, *Bioresour. Technol.*, 130 (2013) 463–471.
- [26] H. Zheng, Z. Wang, J. Zhao, S. Herbert, B. Xing, Sorption of antibiotic sulfamethoxazole varies with biochars produced at different temperatures, *Environ. Pollut.*, 181 (2013) 60–67.
- [27] J.M. Novak, I. Lima, B. Xing, J.W. Gaskin, C. Steiner, K.C. Das, M. Ahmedna, D. Rehrah, D.W. Watts, W.J. Busscher, H. Schomberg, Characterization of designer biochar produced at different temperatures and their effects on a loamy sand, *Ann. Environ. Sci.*, 3 (2009) 195–206.
- [28] F. Suárez-García, A. Martínez-Alonso, J.M.D. Tascón, A comparative study of the thermal decomposition of apple pulp in the absence and presence of phosphoric acid, *Polym. Degrad. Stab.*, 75 (2002) 375–383.
- [29] J.B. Lambert, S. Gronert, H.F. Shurvell, D.A. Lightner, R.G. Cooks, *Organic Structural Spectroscopy*, Prentice Hall, New Jersey, 1998.
- [30] G. Socrates, *Infrared and Raman Characteristic Group Frequencies: Tables and Charts*, John Wiley & Sons Ltd., USA, 1994.
- [31] H. Anjum, T. Murugesan, Effect of functionalization condition on characterization of carbonaceous adsorbent, *Procedia Eng.*, 148 (2016) 1346–1350.
- [32] M.B. Ahmed, J.L. Zhou, H.H. Ngo, W. Guo, M. Chen, Progress in the preparation and application of modified biochar for improved contaminant removal from water and wastewater, *Bioresour. Technol.*, 214 (2016) 836–851.
- [33] F.R. Oliveira, A.K. Patel, D.P. Jaisi, S. Adhikari, H. Lu, S.K. Khanal, Environmental application of biochar: current status and perspectives, *Bioresour. Technol.*, 246 (2017) 110–122.
- [34] G.Z. Kyzas, N.K. Lazaridis, A.C. Mitropoulos, Removal of dyes from aqueous solutions with untreated coffee residues as potential low-cost adsorbents: equilibrium, reuse and thermodynamic approach, *Chem. Eng. J.*, 189–190 (2012) 148–159.
- [35] M.B. Ahmed, J.L. Zhou, H.H. Ngo, W. Guo, Md.A.H. Johir, D. Belhaj, Competitive sorption affinity of sulfonamides and chloramphenicol antibiotics toward functionalized biochar for water and wastewater treatment, *Bioresour. Technol.*, 238 (2017) 306–312.
- [36] M. Jia, F. Wang, Y. Bian, R.D. Stedtfeld, G. Liu, J. Yu, X. Jiang, Sorption of sulfamethazine to biochars as affected by dissolved organic matters of different origin, *Bioresour. Technol.*, 248 (2018) 36–43.
- [37] E. Eren, O. Cubuk, H. Ciftci, B. Eren, B. Caglar, Adsorption of basic dye from aqueous solutions by modified sepiolite: equilibrium, kinetics and thermodynamics study, *Desalination*, 252 (2010) 88–96.
- [38] P. Wang, D. Zhang, H. Zhang, H. Li, S. Ghosh, B. Pan, Impact of concentration and species of sulfamethoxazole and ofloxacin on their adsorption kinetics on sediments, *Chemosphere*, 175 (2017) 123–129.
- [39] X. Lin, J. Zhang, X. Luo, C. Zhang, Y. Zhou, Removal of aniline using lignin grafted acrylic acid from aqueous solution, *Chem. Eng. J.*, 172 (2011) 856–863.
- [40] X. Yu, L. Zhang, M. Liang, W. Sun, pH-dependent sulfonamides adsorption by carbon nanotubes with different surface oxygen contents, *Chem. Eng. J.*, 279 (2015) 363–371.
- [41] H. Chen, B. Gao, H. Li, L.Q. Ma, Effects of pH and ionic strength on sulfamethoxazole and ciprofloxacin transport in saturated porous media, *J. Contam. Hydrol.*, 126 (2011) 29–36.
- [42] X. Han, C. Liang, T.Q. Li, K. Wang, H.G. Huang, X.E. Yang, Simultaneous removal of cadmium and sulfamethoxazole from aqueous solution by rice straw biochar, *J. Zhejiang Univ. Sci. B.*, 14 (2013) 640–649.
- [43] L. Lin, W. Jiang, P. Xu, Comparative study on pharmaceuticals adsorption in reclaimed water desalination concentrate using biochar: Impact of salts and organic matter, *Sci. Total Environ.*, 601–602 (2017) 857–864.
- [44] F. Wang, S. Ma, Y. Si, L. Dong, X. Wang, J. Yao, H. Chen, Z. Yi, W. Yao, B. Xing, Interaction mechanisms of antibiotic sulfamethoxazole with various graphene-based materials and multiwall carbon nanotubes and the effect of humic acid in water, *Carbon*, 114 (2017) 671–678.